

Investigation of phase transitions in NiMn

V. E. Egorushkin, S. N. Kul'kov, and S. E. Kul'kova

Institute of Atmospheric Optics, USSR Academy of Sciences

(Submitted 14 June 1982)

Zh. Eksp. Teor. Fiz. **84**, 599–605 (February 1983)

An experimental and theoretical study is made of the magnetic and structural transformations in NiMn. It is shown that the appearance of an antiferromagnetic structure is due to electron-hole pairing into the triplet state and that iron-doped NiMn has the ferromagnetic properties of an exciton ferromagnet. The structural β - θ transition in NiMn is found to be a striction deformation of the lattice; rhombic striction deformations are observed in a narrow temperature range along with the tetragonal deformations, and their appearance is connected with the topology of the β -NiMn Fermi surface.

PACS numbers: 64.70.Kb, 75.30.Kz, 75.80. + q, 71.35. + z

I. INTRODUCTION

Two transition metals, nickel and manganese, form at temperatures above 700 °C an intermetallic compound in a narrow concentration region near the equiatomic state and with CsCl ordering (β phase). Above 700 °C, manganese nickelide is a paramagnet, and at 710 °C a transition into the antiferromagnetic tetragonal phase is observed in this compound, with a doubled-period structure of the CuAuI type (θ phase).¹

The presently available diagrams of the structural and magnetic states^{2,3} of NiMn differ in the region of the magnetic transformation. Measurements⁴ of the temperature dependence of the thermal expansion and of the lattice constants of θ and β -NiMn pointed to the possible existence of volume magnetostriction in the region of the magnetic transition. However, neither these investigations nor an analysis of the electric resistivity and of the thermoelectric power in different magnetic states⁵ could, naturally, the phase diagram of NiMn more precise.

We report in this paper an experimental study of a structural β - θ transformation by the method of x-ray diffraction and of the magnetic susceptibility of the compounds NiMn and NiMn(Fe) in the magnetic-transition region. We calculate the electronic energy spectrum and the Fermi surface of manganese nickelide in the β phase and construct a theory of phase transformations in this compound.

2. MATERIALS AND INVESTIGATION TECHNIQUE

The alloys (see Table I) were prepared in an induction furnace and the composition was monitored by chemical analysis. X-ray diffraction investigations were carried out with a DRON-2 diffractometer with the UVD-2000 high-

TABLE I. Composition of investigated alloys (at. %)

Number of alloy	Ni	Mn	Fe	$n=s+d$, electrons/atoms
1	49.5	50.5	—	8.48
2	48.6	47.2	4.2	8.50
3	48.8	45.8	5.6	8.52
4	50	40.3	9.7	8.60

temperature attachment. Samples were prepared in the form of 20×10×10 mm plates. The magnetic susceptibility was measured by the Faraday method in a field 2.5 kOe.

To vary the electron density, the alloys were doped with a third component, iron, which does not change, according to Ref. 5, the sequence of the structural transformations, but alters substantially the magnetic state of the alloy.

The procedure used to calculate the electronic band structure of NiMn is described in Ref. 6. To construct the Fermi surface, the electron spectrum was calculated in 32 planes parallel to the ΓXM plane of the Brillouin zone (BZ) in intervals of 1/64 of the wave vector k . The spectrum was refined by a linear interpolation or by recalculating the spectrum with smaller intervals.

3. RESULTS AND DISCUSSION

The temperature dependences of the lattice parameters of all the phases produced in the equiatomic alloy NiMn are shown in Fig. 1. The sequence of the transformations and the crystal-lattice parameters of the γ , β , and θ phases agree well with the data of Refs. 2–4. However, in the temperature region 500–700 °C the x-ray diffraction patterns reveal near the (111) reflection of the θ phase of NiMn a weak line that

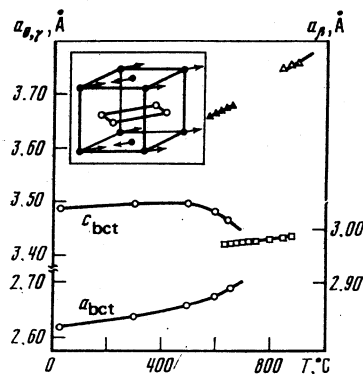


FIG. 1. Temperature dependences of the parameters of the lattices of all the phases of the alloy No. 1: \circ - θ , \square - β , \triangle - γ , \blacktriangle - γ' (inset—crystal and magnetic cells of the θ -NiMn alloy, the atoms are designated: \bullet —Mn, \circ —Ni).

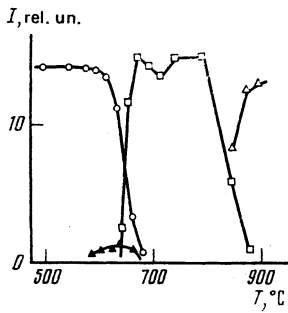


FIG. 2. Temperature dependences of the integrated intensities of the lines of alloy No. 1 (the notation is the same as in Fig. 1).

belongs to neither of the known phases of NiMn. Its relative intensity compared with the main lines is very low (Fig. 2), and its characteristic feature is that the temperature dependence of the interplanar distance corresponding to this line is an exact continuation of the temperature dependence of the interplanar distance of the (111) line of the γ phase of NiMn.

Figure 3 shows the results of the measurement of the magnetic susceptibility of a number of alloys. All the curves have a sharp peak at a temperature corresponding to the Neel temperature T_N . At the same time, in the alloys whose electron density exceeds 8.5 electrons/atom, at temperatures below T_N , an anomalous decrease of the susceptibility with increasing temperature is observed, something quite untypical of antiferromagnets. Moreover, in this temperature interval the magnetic susceptibility obeys the Curie-Weiss law. The result were processed in analogy with Ref. 7 and it was found that in alloys with an average electron density more than 8.5 electrons/atom an average magnetic moment appears and is proportional to the iron concentration (see the inset of Fig. 3); the average magnetic moment does not exceed 1 Bohr magneton.

4. THEORY OF PHASE TRANSITIONS

We begin with a discussion of the transitions with the more general case of NiMn(Fe) alloys. The small magnetic

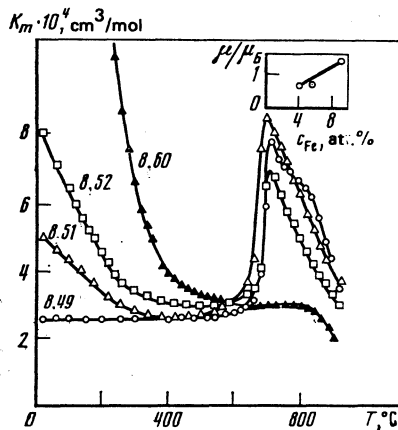


FIG. 3. Temperature dependences of the magnetic susceptibility of the alloys: \circ — No. 1, \triangle — No. 2, \square — No. 3, \blacktriangle — No. 4; the numbers at the curves are the electron density in electrons per atoms (inset—dependence of the magnetic moment on the iron content in the alloy).

moment in the low-symmetry phase of NiMn(Fe) (Fig. 3), the strong dependence of the magnetic properties of the doped manganese nickelide on the electron density, and also the presence of a structural transformation together with a magnetic one allow us to assume that we are dealing with excitonic ferromagnetism,⁸⁻¹⁰ the appearance of a nonzero total magnetic moment in T_e is due to the moving apart of the Fermi surfaces of the electrons and holes at a given value of their densities and to the lifting of the spin degeneracy of the electron and hole bands. In undoped NiMn the presence of additional sections of the Fermi surface do not permit establishment of a density difference, and the undoped compound does not exhibit ferromagnetic properties.

To describe the transformations we consider a compound that is unstable with respect to doubling of the period, and with a spectrum satisfying the conditions $\varepsilon_i(\mathbf{k}) = -\varepsilon_i(\mathbf{k} + \mathbf{Q})$ near the Fermi energy. The vector \mathbf{Q} is equal to half the reciprocal-lattice vector. The subsequent analysis must be carried out in analogy with Refs. 9 and 10, using the Hamiltonian

$$H = H_0 + H_{ee} + H_{ep} + H_{\xi}, \quad (1)$$

where H_0 is the Hamiltonian of the noninteracting electrons and phonons H_{ee} is the Hamiltonian of the Coulomb interelectron interaction, H_{ep} is the operator of the interaction of the electrons with the phonons at the point \mathbf{Q} , and $H_{\xi} = -\mu \mathbf{H} \cdot \boldsymbol{\sigma}$ is the Zeeman Hamiltonian which is needed for the calculation of the contribution to the magnetic susceptibility. The explicit form of (1) and all the symbols are analogous to those in Refs. 9 and 10. The possibility of doping NiMn can be taken into account with the aid of the chemical potential μ that characterizes the change in the occupation of the bands $\varepsilon(\mathbf{k})$.

It is shown in Refs. 8-10 that the appearance of excitonic ferromagnetism is formally due to the fact that the anomalous intraband Green's functions $G_{jj}^{\alpha-\alpha}(\mathbf{k}, 0)$, where α is the spin index and determines the value of the local moment, are not equal to zero when the magnetic and structural order parameters Δ_t and Δ_s exist simultaneously. In this case the equations that relate the singlet Δ_s and the triplet Δ_t order parameters can be obtained by simultaneous solution of the system of equations for the matrix temperature Green's functions and the self-consistency conditions at $g_t > g_s$ (where g_t and g_s are respectively the triplet and singlet coupling constants) and the conservation condition for the total electron density n .

Using next the Landau functional far from the transition point

$$F = -4\mu_B N_0 \frac{\partial I(0, n)}{\partial n} \\ \times \Delta_s \Delta_t H - \alpha_1 \Delta_s^2 - \alpha_2 \Delta_t^2 + \frac{1}{2} \beta_1 (\Delta_s^4 + \Delta_t^4) + \beta_2 \Delta_s^2 \Delta_t^2, \\ \beta_1 - \beta_2 \gg \alpha_2 \quad (2)$$

and minimizing it with respect to Δ_s and Δ_t , we find¹⁰ that below the antiferromagnetic transition temperature the contribution to the magnetic susceptibility, connected with the

appearance of the singlet gap, has a Curie-Weiss form and becomes singular when the condition

$$\ln(\Delta_{i0}/\Delta_{i0}) = 2\Delta_i^2 \partial I(\Delta_i, n) / \partial (\Delta_i^2) \quad (3)$$

is satisfied, i.e., the antiferromagnetic phase becomes unstable with respect to the charge-density wave (the parameter Δ_s). Spontaneous magnetic moment is produced in the system, and excitonic ferromagnetism exists in the (Δ_s, Δ_i) plane.

In expressions (2) and (3) N_0 is the state density on the Fermi level, Δ_{s0} and Δ_{i0} are the equilibrium values of the order parameters at $T = 0$ and $n = 0$,

$$I(\Delta_i, n) = \int_0^{\infty} d\varepsilon \left[\frac{f(-E-n) - f(E-n)}{E} \right]_{i+} \left[\frac{f(\varepsilon) - f(-\varepsilon)}{\varepsilon} \right],$$

$E = (\varepsilon^2 + \Delta_i^2)^{1/2}$, and $f(\varepsilon)$ is the Fermi distribution function.

At equal coupling constants, the ferromagnetic solution

$$\Delta_i^2 = \Delta_s^2 = \alpha / (\beta_1 + \beta_2), \quad F_f = -\alpha / (\beta_1 + \beta_2)$$

is favored over the antiferromagnetic solution

$$\Delta_s = 0, \quad \Delta_i = \alpha / \beta_1, \quad F_{af} = -\alpha / 2\beta_1,$$

i.e., the high-temperature phase, doped such that $g_s = g_i$, can immediately go over into the paramagnetic phase (which goes over into the ferromagnetic phase at T_c), bypassing the antiferromagnetic transition. A similar solution in NiMn(Fe) corresponds to alloy No. 4 in Table I.

In the absence of doping, only a triplet order parameter Δ_i is produced in NiMn, i.e., a spin-density wave (SDW)

$$\rho(\mathbf{r}) = \rho(\mathbf{Q}) \cos(\mathbf{Q}\mathbf{r}) \quad (4)$$

and antiferromagnetic ordering at the Neel temperature

$$T_i = (1.78/\pi) \Delta_{i0}, \quad \Delta_{i0} = \omega \exp(-1/g_i N_0),$$

where ω is a cutoff energy lower than the Fermi energy, $\omega \ll \omega_F$. Estimates at $T_i \sim 1000$ K and $\omega \sim 1$ eV (bearing in mind that $\varepsilon_F \approx 10$ eV) yield the reasonable value $g_i N_0 \sim 1$.

In (4), \mathbf{Q} is the SDW wave vector and determines the period of the magnetic structure. To find \mathbf{Q} it is necessary to use the band spectrum $\varepsilon(\mathbf{k})$ of the NiMn compound. The calculation of $\varepsilon(\mathbf{k})$ is described in detail in Ref. 6, where the band spectrum is used also to calculate the temperature dependences of the electric resistivity and the thermoelectric power of β -NiMn. The good agreement between the theoretical and experimental data is evidence of the proximity of the calculated $\varepsilon(\mathbf{k})$ to the real electron spectrum of the compound.

It can be seen from Fig. 1 (Ref. 6) that the typical "excitonic" section of the spectrum is the section $R - X$. According to Ref. 11, a parabolic hole band, in this case at the point R , and a similar electron band at the point X , can become paired into the triplet state, and this leads to an antiferromagnetic order. In other words, for β -NiMn the condition $\varepsilon(\mathbf{k}) = -\varepsilon(\mathbf{k} + \mathbf{Q})$ is satisfied around the point R of the Brillouin zone (BZ) for the hole section of the Fermi surface and around the X point the electronic section; the vector \mathbf{Q} that connects these points is equal to half the reciprocal-lattice vector: $\mathbf{Q} = (\pi/a)(110)$. The period of the magnetic struc-

ture, determined by the vector \mathbf{Q} , is such that the SDW polarization vector does not change direction at the lattice sites along the z axis and in the XY direction, but reverses sign at the site along the axes X and Y .

This structure with oppositely directed magnetic moments of the Mn atoms and with zero moment of Ni, shown in the inset of Fig. 1, coincides with the experimentally observed¹² antiferromagnetic structure of the θ phase of NiMn.

The reason why only the Mn atoms have a moment is that all the electrons of the "excitonic" band belong only to Mn, so that the representations R'_{12} , X'_3 , and S_2 (see Fig. 1 of Ref. 6) correspond to the Mn terms; this can be easily verified by the appropriate group-theoretical classification of the electronic states of the atoms located at two different sites of the β -phase of NiMn.

To describe the structural distortions that accompany the magnetic transformation in undoped NiMn, we include in the Hamiltonian, in place of the missing electron-phonon interaction in the "displacement" channel ($\Delta_s = 0$), the interaction of the electrons of the $X'_3 - R'_{12}$ band with the phonons in the "deformation" channel:

$$H_\varepsilon = \sum_{\mathbf{k}, i} q_k \eta a_{i1}^+(\mathbf{k}) a_{2i}(\mathbf{k}), \quad (5)$$

where q_k is the interband component of the deformation potential, $i = 1, 2, 3$, and in the basis of the R'_{12} representation we have

$$\eta = \eta_1 + i\eta_2, \quad \eta_1 = \varepsilon_{xx} + \varepsilon_{yy} - 2\varepsilon_{zz}, \quad \eta_2 = \sqrt{3}(\varepsilon_{xx} - \varepsilon_{yy}),$$

where ε_{ii} are the components of the strain tensor.

It is now easy to write the contribution made to the free energy by the deformation order parameter, in the form of an expansion in invariants far from the transition point:

$$F_\eta = \alpha_\eta (\eta_1^2 + \eta_2^2) + \beta \eta_1 (\eta_1^2 - 3\eta_2^2) + \gamma (\eta_1^2 + \eta_2^2)^2. \quad (6)$$

The free-energy contribution that is mixed in η and Δ_i and is linear in η takes, when account is taken of $\Delta_i = \Delta_{si}$, the form

$$F_{\eta\Delta_i} = \kappa \eta_1 \Delta_{si}^2. \quad (7)$$

Minimizing $F_\eta + F_{\eta\Delta_i}$ with respect to η we obtain for tetragonal deformation ($\varepsilon_{xx} = \varepsilon_{yy} = -\varepsilon_{zz}/2$)

$$\eta_1 = [(\alpha_\eta^2 - 3\beta\kappa\Delta_{si}^2)^{1/2} - \alpha_\eta] / 3\beta, \quad \eta_2 = 0. \quad (8)$$

It is clear from (8) that the deformation η_1 is of striction origin. Substituting in (8) the solution with the SDW, $\Delta_i^2 = \alpha_2/\beta_1$, we obtain the temperature dependence

$$\eta_1(T) \sim [(T_i - T)/T_i]^{1/2},$$

which agrees with the experimental temperature dependence 4 of the bulk magnetostriction; the striction deformation is in this case negative. As a result, the cubic lattice is stretched along the Z axis and $c = a_0(1 - \eta_1/3)$ increases with decreasing temperature, whereas $a = a_0(1 + \eta_1/6)$ decreases (Fig. 1).

5. FERMI SURFACE AND RHOMBIC DISTORTIONS IN NiMn

The total Fermi surface of NiMn was reconstructed by us with the aid of interactions with the planes $k_z = \text{const}$ in

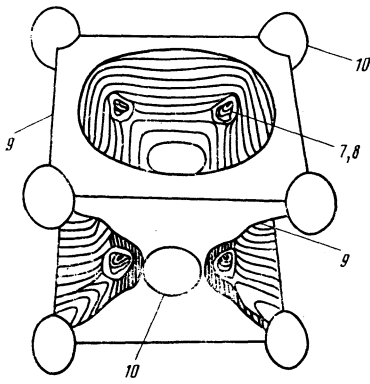


FIG. 4. Fermi surface of β -NiMn (electronic).

steps of $1/64$ and $1/128$ in k . An analysis of the sections and a study of the Fermi surface constructed with their aid (Fig. 4) shows that NiMn has four Fermi-surface sheets corresponding to four energy bands that cross the Fermi level.

The surface corresponding to the energy band 9, centered about the point M of the Brillouin zone, is an open electron surface with complicated topology whose sections decrease in area with increasing k_z . The Fermi-surface sheet corresponding to the energy band 10 is a closed ellipsoidal energy band, is centered at the point X and has one extremal section in the plane $k_z = 0$. The surfaces corresponding to the energy bands 7 and 8 are also closed surfaces located near the midpoint of the Λ direction of the Brillouin zone. The volume of these Fermi-surface regions is small compared with the volumes corresponding to the energy bands 9 and 10.

Figure 5 shows a superposition of the Fermi-surface regions centered at the point R and X . In this case the Fermi-surface regions centered near the Brillouin zones Γ and M become congruent. The new plane produced as a result of the congruence leads to a splitting of small parts of the Fermi surface near the direction of Λ . Therefore an x-ray structural analysis should reveal a satellite corresponding to a new plane that does not coincide with the $(\pi/2a)(111)$ plane of the θ phase.

This was precisely the line observed by us in experiment (Fig. 2). Indeed, the calculated value of the length from the

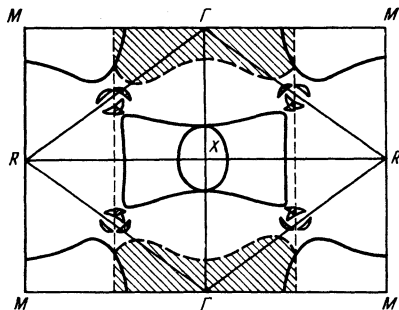


FIG. 5. Sections of the Fermi surface of NiMn (the Fermi surface regions produced as the result of the congruences $X-R$ and $\Gamma-M$ are shown shaded).

point Γ to the center of gravity of these regions, equal to 0.48 \AA^{-1} , agrees well with the experimental value $d_{hkl} = 0.46 \text{ \AA}^{-1}$. The low intensity of this reflection is due to the small amplitude of the SDW.

A calculation of the Fermi surface with the lattice parameter extrapolated to lower temperatures does not reveal these regions (Fig. 4b of Ref. 6). It appears that this is why the satellite vanishes with decreasing temperature.

Since the states that form these regions of the Fermi surface have a symmetry close to the states of the term Λ_3 (Fig. 1 of Ref. 6), by using the method of invariants¹³ it is easy to construct the free energy as a function of the strains, of the magnetic field, etc. and to calculate the thermal expansion $\alpha(T)$ of the lattice. It turns out in this case that in the free energy the first-order terms, which are linear in the strains, contain components of the magnetic-field intensity vector H .

Calculating the electronic contribution to $\alpha(T)$, we have

$$\alpha_{ii} = (-1)^i D H_i / T (2C_{12} - C_{11}),$$

where $i = 1, \text{ and } 2$; D is a positive constant; C_{12} and C_{11} are the elastic moduli of the equilibrium lattice.

Thus, the observed reflection (Fig. 2) near the (111) plane of θ -NiMn is connected with striction rhombic distortions of the initial cubic lattice. These distortions, just as the tetragonal ones (8), correspond to nondegenerate rhombic solution of the equations for the minimization of the functional (6), (7):

$$\eta_1 = 0, \quad \eta_2 = \kappa \Delta_z^2 / 3\beta.$$

CONCLUSIONS

1. Manganese nickelide doped with iron in such a way that the electron density exceeds 8.5 electrons/atom exhibits paramagnetic properties and the observed ferromagnetism is of excitonic origin.

2. We calculated the electron energy spectrum and the Fermi surface of β -NiMn and have shown that the appearance of antiferromagnetism in NiMn is a consequence of the instability of the metal to SDW. The phase of the SDW was obtained and the magnetic structure of the antiferromagnetic phase was determined.

3. A more accurate phase diagram of manganese nickelide was experimentally obtained in the region of the magnetic transformation.

A satellite of the structure reflection (111) was observed and it was shown that it is due to rhombic distortions that accompany the β - θ transformation.

4. We have shown that the structural tetragonal and rhombic distortions are of striction origin.

In conclusion, the authors wish to thank V. A. Volkov, N. I. Kulikov, and V. V. Tugushev for a discussion of the work.

¹E. Kren and L. Pal, J. Phys. Chem. Sol. 26, 101 (1968).

²B. R. Coles and W. J. Hume-Rothery, Inst. Metals 80, 85 (1951).

³K. E. Tsiplakis and E. Kneller, Metallkunde 60, 433 (1969).

⁴S. N. Kulkov, V. S. Demidenko, and V. E. Panin, Phys. Stat. Sol. (a) 60, K55 (1980).

- ⁵S. N. Kul'kov, V. S. Demidenko, and V. E. Panin, in: *Élektronnoe stroenie i fizikokhimicheskie svoïstva tugoplavkikh soedineniï i splavov* (Electron Structure and Physicochemical Properties of Refractory Compounds and Alloys), Naukova Dumka, Kiev, 1980, p. 233.
- ⁶I. N. Anokhina, V. E. Egorushkin, S. N. Kul'kov, S. E. Kul'kova, and V. P. Fadin, *Izv. vyssh. ucheb. zaved., Fizika*, No. 10, 23 (1981).
- ⁷J. Pop and A. Guergui, *Phys. Stat. Sol. (b)* **88**, 181 (1978).
- ⁸B. A. Volkov and Yu. V. Kopaev, *Pis'ma Zh. Eksp. Teor. Fiz.* **19**, 168 (1974) [*JETP Lett.* **19**, 104 (1973)].
- ⁹B. A. Volkov, Yu. V. Kopaev, and A. I. Risunov, *Zh. Eksp. Teor. Fiz.* **68**, 1899 (1975) [*Sov. Phys. JETP* **41**, 952 (1975)].
- ¹⁰B. A. Volkov and A. I. Risunov, *ibid.* **70**, 1130 (1976) [**43**, 589 (1976)].
- ¹¹A. P. Kozlov and L. A. Maksimov, *ibid.* **48**, 1184 (1965) [**21**, 790 (1965)].
- ¹²J. S. Kasper and J. S. Kouvel, *J. Phys. Chem. Sol.* **11**, 231 (1959).
- ¹³G. Bir and G. Pikus, *Symmetry and Strain-Induced Effects in Semiconductors*, Wiley, 1975, [Russ. orig. Nauka, 1972, Chap. 4, p. 304].

Translated by J. G. Adashko